Monthly Notices of the ROYAL ASTRONOMICAL SOCIETY

MNRAS **529,** 52–58 (2024) https://doi.org/10.1093/mnras/stae442
Advance Access publication 2024 February 13

Examining the self-interaction of dark matter through central cluster galaxy offsets

D. Cross [1,2,3★] G. Thoron,[1,2★] T. E. Jeltema [1,2★] A. Swart,[1,2,4] D. L. Hollowood,[1,2] S. Adhikari [5] S. Bocquet,[6] O. Eiger,[1,2,7] S. Everett,[8] J. Jobel,[1,2] D. Laubner,[1,2] A. McDaniel,[9] M. Aguena,[10] O. Alves,[11] F. Andrade-Oliveira,[11] D. Bacon,[12] E. Bertin,[13,14] D. Brooks,[15] D. L. Burke,[16,17] A. Carnero Rosell,[10,18,19] M. Carrasco Kind,[20,21] R. Cawthon,[22] M. Costanzi,[23,24,25] L. N. da Costa,[10] M. E. S. Pereira,[26] T. M. Davis,[27] S. Desai,[28] P. Doel,[15] I. Ferrero,[29] J. Frieman,[30,31] J. García-Bellido,[32] G. Giannini,[33] D. Gruen,[34] R. A. Gruendl,[20,21] S. R. Hinton,[27] K. Honscheid,[35,36] D. J. James,[37] K. Kuehn,[38,39] J. L. Marshall,[40] J. Mena-Fernández,[41] F. Menanteau,[20,21] R. Miquel,[33,42] R. L. C. Ogando,[43] A. Pieres,[10,43] A. A. Plazas Malagón,[44] M. Raveri,[45] A. K. Romer,[46] E. Sanchez,[41] I. Sevilla-Noarbe,[41] M. Smith,[47] M. Soares-Santos,[11] F. Sobreira,[10,48] E. Suchyta,[49] M. E. C. Swanson,[50] G. Tarle,[11] C. To,[35] N. Weaverdyck,[11,51] J. Weller,[52,53] and P. Wiseman[47] (DES Collaboration)

Affiliations are listed at the end of the paper

Accepted 2024 February 7. Received 2024 February 7; in original form 2023 April 20

ABSTRACT

While collisionless cold dark matter models have been largely successful in explaining a wide range of observational data, some tensions still exist, and it remains possible that dark matter possesses a non-negligible level of self-interactions. In this paper, we investigate a possible observable consequence of self-interacting dark matter: offsets between the central galaxy and the centre of mass of its parent halo. We examine 23 relaxed galaxy clusters in a redshift range of 0.1–0.3 drawn from clusters in the Dark Energy Survey and the Sloan Digital Sky Survey which have archival *Chandra* X-ray data of sufficient depth for centre and relaxation determination. We find that most clusters in our sample show non-zero offsets between the X-ray centre, taken to be the centroid within the cluster core, and the central galaxy position. All of the measured offsets are larger, typically by an order of magnitude, than the uncertainty in the X-ray position due to Poisson noise. In all but six clusters, the measured offsets are also larger than the estimated, combined astrometric uncertainties in the X-ray and optical positions. A more conservative cut on concentration to select relaxed clusters marginally reduces but does not eliminate the observed offset. With our more conservative sample, we find an estimated median X-ray to central galaxy offset of $\mu = 6.0^{+1.4}_{-1.5}$ kpc. Comparing to recent simulations, this distribution of offsets is consistent with some level of dark matter self-interaction, though further simulation work is needed to place constraints.

Key words: galaxies: clusters: general – cosmology: dark matter – X-rays: galaxies: clusters.

1 INTRODUCTION

The cold dark matter (CDM) paradigm postulates that dark matter is non-relativistic and collisionless. This model has been very successful in predicting the large-scale structure of the universe (Davis et al. 1985; Springel et al. 2005). However, potential discrepancies exist between theory and observations, particularly at smaller scales (for reviews, see e.g. Weinberg et al. 2015; Bullock & Boylan-Kolchin 2017; Buckley & Peter 2018). In addition, despite multipronged searches for CDM candidates, a conclusive non-gravitational signal has not been found, and basic tenants of the CDM paradigm, like dark matter's collisionless nature, are not yet strongly constrained (e.g. Tulin & Yu 2018).

A generic possibility is that there may be undiscovered forces between dark matter particles; in this case, dark matter would possess non-zero self-interactions and not be collisionless. Termed self-interacting dark matter (SIDM), this model was initially proposed as a solution to the core-cusp problem (Spergel & Steinhardt 2000). However, some form of self-interaction is a generic beyond CDM possibility and a common feature of dark sector theories, and SIDM models predict potentially observable consequences for the shapes, densities, and substructure of dark matter haloes (see e.g. reviews by Tulin & Yu 2018; Adhikari et al. 2022).

★ E-mail: dane.cross2016@gmail.com (DC); gthoron@ucsc.edu (GT); tesla@ucsc.edu (TEJ)

One important discrepancy between CDM simulations and observations is that the central circular velocity in galaxies is much lower than the velocities predicted by dark-matter-only simulations (e.g. Casertano & van Gorkom 1991; Flores et al. 1993). Termed the 'core/cusp problem', CDM predicts a sharper density peak in the centres of dark matter haloes, scaling as $\rho_{\rm DM} \propto r^{-1}$ (e.g. Dubinski & Carlberg 1991; Navarro, Frenk & White 1996, 1997), than actually occurs with the data favouring constant density cores, particularly for low surface brightness and dwarf galaxies. (e.g. Flores & Primack 1994; Moore 1994; Burkert 1995; de Blok, McGaugh & Rubin 2001a; de Blok et al. 2001b; Kuzio de Naray, McGaugh & de Blok 2008). The inclusion of baryonic physics in hydrodynamical simulations and in particular supernova feedback goes a long way toward resolving the core/cusp discrepancy with simulations able to produce cores at least in some mass ranges (e.g. Governato et al. 2010; Oh et al. 2011; Zolotov et al. 2012). However, it is unclear if baryonic effects alone can produce the full diversity of density profiles observed (e.g. Kuzio de Naray et al. 2010; Oman et al. 2015). See also Tulin & Yu (2018), Adhikari et al. (2022), and references therein for discussion of the core/cusp problem and potential solutions.

Another possibility is that properties of the dark matter which deviate from the assumptions of CDM lead to the lower observed central densities. As already mentioned, SIDM is one potential solution (e.g. Spergel & Steinhardt 2000) in which self-interactions lead to heat transfer from outer, hotter regions to cooler, inner regions giving a uniform inner velocity dispersion and reduced central density. Simulations have shown that SIDM plus baryons can naturally lead to the observed diversity in galaxy rotation curves and central densities (Creasey et al. 2017; Kamada et al. 2017; Ren et al. 2019; Zavala et al. 2019). We note that other dark matter models have also been proposed that may produce cores and fix the observed small-scale issues, including warm dark matter (e.g. Bode, Ostriker & Turok 2001; Viel et al. 2013), wave or fuzzy dark matter (e.g. Hu, Barkana & Gruzinov 2000; Hui et al. 2017; Hui 2021), and superfluid dark matter (e.g. Khoury 2016).

These different dark matter models may be distinguished by the scale dependence of their effects (Buckley & Peter 2018). In addition, on the particle theory side, many models for SIDM naturally lead to a dark matter self-interaction cross-section over mass ($\sigma_{\rm DM}/m$) that depends on the relative velocity of the dark matter particles (e.g Tulin & Yu 2018; Adhikari et al. 2022, and references therein), and a velocity-dependent cross-section is preferred when reconciling dwarf galaxy observations with constraints on the scale of clusters of galaxies in an SIDM context (e.g. Kaplinghat, Tulin & Yu 2016). In this paper, we turn our attention to the most massive end of structure formation, clusters, and a recently proposed observational consequence of SIDM and central cores in general.

Using two component simulations (modelling dark matter and galaxies), Kim, Peter & Wittman (2017) find that in SIDM models CCGs oscillate on long-lived orbits out to radii of 100 kpc or more and for up to Gyrs following a merger, likely even when clusters appear otherwise relaxed. In the CDM paradigm, the halo's peaky density distribution will cause the central cluster galaxy (CCG) to be very near the halo centre of mass. Conversely, in the SIDM paradigm the CCG will typically be offset from the dark matter centre of mass due to the larger orbits expected in a shallower density distribution. The average offset from the centre of mass is dependent on the halo core size, and thus for different cross-sections, the offset distribution will be different (Kim et al. 2017). Including the effects of baryons using the BAryons and HAloes of MAssive Systems (BAHAMAS) simulations, Harvey et al. (2019) find much smaller, but observable offsets of the CCGs even in relaxed clusters with a median offset that increases with the SIDM cross-section. Using a sample of 10 strong lensing clusters, they derive a limit on the cross-section of $\sigma/m < 0.4$ cm^2 g^{-1}.

In this paper, we look for offsets of the central galaxy in 23 galaxy clusters selected to be both relaxed and X-ray bright. We estimate the position of the centre of mass using the X-ray data, specifically the X-ray centroid within the core region, comparing them to the position of the CCG. In Section 2, we discuss our methodology including cluster selection and relaxation criterion and cluster centre determination. Section 3 presents our results, and in Section 4, we discuss the consequences and limitations of our analysis. In this work, we assume a flat lambda-CDM cosmology with $H_0 = 67.7$ km (Mpc s)$^{-1}$ and $\Omega_m = 0.31$.

2 DATA REDUCTION AND METHODOLOGY

2.1 Cluster data

We select clusters from two large area surveys, the Dark Energy Survey (DES, DES Collaboration 2005) and the Sloan Digital Sky Survey (SDSS, Eisenstein et al. 2011), specifically DES Y3 Gold (Sevilla-Noarbe et al. 2021) and SDSS DR8 (Aihara et al. 2011). Clusters were identified in the photometric survey data using the red-sequence Matched-filter Probabilistic Percolation cluster finder (REDMAPPER) algorithm Rykoff et al. (2014, 2016). REDMAPPER selects clusters based on overdensities of galaxies in colour space. More specifically, it identifies cluster members based on the red sequence, iteratively determining both the cluster centre and the cluster red sequence. Potential member galaxies in a given cluster are given a membership probability weighted by a matched filter based on colour, magnitude, and separation distance from the estimated cluster centre (taken to be the most probable identified CCG). In this work, we use the SDSS REDMAPPER v.6.3.1 and DES Y3 REDMAPPER 6.4.22+2 catalogues with richness $\lambda > 20$, and central galaxy positions were taken from these catalogues. Where both surveys overlap and had centre galaxy positions for the same cluster, we removed the positions from the SDSS catalogue and kept the positions from DES Y3.

As described below, we use the X-ray brightness distribution to both select relaxed clusters and to estimate the cluster centre of mass. For this reason, our sample was limited to clusters with existing high spatial resolution *Chandra* X-ray data. The *Chandra* data were reduced using the Mass Analysis Tool for Chandra pipeline (MATCha, Hollowood et al. 2019). For an input cluster catalogue, MATCha reduces any existing *Chandra* data and determines cluster temperature and luminosity within several radii as well as finding the X-ray centroid and peak positions. The SDSS X-ray analysis is described in Hollowood et al. (2019) and the DES Y3 analysis in Kelly et al. (in preparation). In this work, we re-derive centre locations starting from the reduced data as described in the next section. Central galaxy positions are taken from the DES or SDSS catalogues. In some cases, REDMAPPER identifies the wrong galaxy as the central galaxy (Hollowood et al. 2019; Zhang et al. 2019); for these clusters we identify the correct central galaxy based on proximity to the X-ray centre and take the position of the correct central from the optical catalogues.

2.2 Cluster selection

Beginning with the full DES and SDSS REDMAPPER catalogues, we make a series of cuts to select a sample of clusters to perform our analysis on. We need robustly X-ray-detected clusters with high resolution, so we select clusters with redshifts between 0.1 and 0.3. The lower redshift limit is set by the requirement that the cluster X-ray emission fit within the *Chandra* field of view, while the upper redshift limit is set by the need to resolve positions to within a few kpcs. For the signal-to-noise ratio of the X-ray data, we require a minimum ratio of 25 from the *Chandra* data in a 500 kpc radius region to ensure that the noise does not dominate the uncertainty in the centre determination.

As we will be using the X-ray emission as a tracer of the cluster centre, we also select relaxed clusters where we expect the X-ray peak to trace fairly well the centre of the gravitational potential. The selection of relaxed clusters is made based on the X-ray concentration. The concentration is calculated by taking a ratio of the exposure-corrected photon counts within a radius of 15 per cent of the R_{500} radius around the peak of X-ray emissions and in an annular region that extended from $0.15R_{500}$ to R_{500}. This means that for a given concentration c, the number of photon counts within $0.15R_{500}$ radius c times the number of counts in the annulus $0.15R_{500} < R < R_{500}$.

Thus, higher concentration c means a higher amount of mass in the centre of the cluster. We excluded observations in which the R_{500} distance was greater than the area covered by the observation. The R_{500} radius is the radius within which the average density of the cluster is 500 times larger than the critical density of the universe, and here we estimate R_{500} from the X-ray temperature as in Hollowood et al. (2019). We select clusters with concentrations of 0.5 or higher. This resulted in a final sample of 23 clusters.

Our definition of concentration differs somewhat from that of previous works as our definition relies on the R_{500} radius. In particular, the criterion used by Harvey et al. (2019) to select relaxed clusters in SIDM simulations was defined by a core radius of 100 kpc and an outer radius for the annulus of 300 kpc. As we are looking at galaxy clusters with a range of masses and size, defining the concentration based on an overdensity radius like R_{500} allows us to more consistently compare statistics for both large and small galaxy clusters. Despite the difference in these criteria, the two concentration definitions are highly correlated; we find that the minimum concentration of 0.2 used in Harvey et al. (2019) corresponds roughly to a concentration of 0.44 for our R_{500}-based concentration definition. After visual examination, we chose to make a slightly more conservative cut on concentration of 0.5 or greater. This gives a sample of 23 clusters; for comparison using the concentration definition of Harvey et al. (2019) and their cut on concentration greater than 0.2 would have resulted in a sample of 28 clusters. Our visual examination showed that some clearly merging clusters would remain in the sample under the Harvey et al. (2019) cut. Even for our slightly more conservative cut, one clear merger remains, and in Section 3 we explore a cut on concentration greater than 0.6 to address this.

2.3 Determination of cluster centre

The final part of the data reduction is the determination of the cluster centre to be compared to the DES or SDSS central galaxy positions. In this work, we define the cluster centre to be the X-ray centroid determined within the cluster core, as described below. As we have selected relaxed clusters, we expect the X-ray distribution to trace the underlying gravitational potential and thus mass distribution.

Specifically, we define the cluster centre to be the centroid of the X-ray emission within a radius of $0.15R_{500}$. This process requires that the initial centre of the R_{500} aperture be a good first-order approximation to the actual centroid. The MATCha algorithm approximates the X-ray peak position as the brightest pixel in the point-source subtracted, smoothed X-ray image. In order to improve this approximation, we created an iterative algorithm that measures the centroid of the $0.15R_{500}$ aperture; after centroid determination we then use this centroid as the new centre of the circle and recalculate the centroid until the difference between the iterations is less than two pixels.

In order to quantify the uncertainties in the centroid measurement, we resampled the image to generate a new realization of the noise and then remeasured the centroid and its offset from the central galaxy in the simulated image. To generate noise, we drew a random number from a Poisson distribution for each pixel, where the mean value of the Poisson distribution for each pixel was taken to be the original pixel value in the image. We repeated this process 100 times, and took the median centroid to CCG offset as our accepted value, with a confidence interval defined as the range between the 16th and 84th smallest offsets.

3 RESULTS

Results for the 23 clusters with concentrations greater than 0.5 are shown in Table 1. The central galaxy offsets range from 1.5 to 120 kpc, with most falling in between 4 and 15 kpc. The errors on these measurements are around an order of magnitude smaller than the measurements themselves, ranging from 0.1 to 1.0 kpc, with most falling between 0.1 and 0.4 kpc. Note that the size of the measured offsets are generally larger than but comparable to the pixel size and on-axis *Chandra* resolution of ∼0.5 arcsec; we discuss the positional uncertainties further in Section 4.

Following Harvey et al. (2019), we fit the central galaxy offset distribution to a lognormal probability density function with the form

$$f(x|\sigma,\mu) = \frac{1}{x\sigma\sqrt{2\pi}} \exp\left(-\frac{1}{2\sigma^2}\ln^2\left(\frac{x}{\mu}\right)\right),$$

using the maximum-likelihood estimator from the SCIPY library, which finds the σ and μ values that maximize

$$\mathcal{L}(\sigma,\mu) = \prod_{k=1}^{n} f(x_k|\sigma,\mu),$$

where x_k is the kth offset in our set of measured offsets. Both the offset distribution and fit are shown in Fig. 1. For the lognormal fit with our nominal concentration cut of 0.5, we find a median value $\mu = 7.9 \pm 1.6$ kpc and $\sigma = 0.9 \pm 0.2$. Errors on the fit parameters were estimated using bootstrapping with a total of 100 000 trials. The parameter values, along, with their errors, are shown in Table 2.

Of the nominal sample of 23 clusters the measured offsets are typically 20 kpc or less with the exception of AS0592. This cluster has an offset that is one to two orders of magnitude larger than the rest of the sample. AS0592 is a known merger (Botteon, Gastaldello & Brunetti 2018), and an examination the X-ray images of AS0592 showed two X-ray substructures and two possible CCGs in the cluster. For a lognormal fit of the data with just this outlier removed, the median value of this set of clusters is 7.0 kpc. However, the fact that this concentration let in a merger at all implies that the 0.5

Table 1. Offsets of the CCG from the X-ray centre and associated errors. Tabulated is the cluster name (column 1), the survey from which the cluster was drawn (column 2), the *Chandra* obsID (column 3), the REDMAPPER redshift (column 4), the CCG to X-ray offset (column 5), the uncertainty in the offset due to Poisson noise (column 6), the X-ray concentration (column 7), and the physical size corresponding to the estimated, combined positional uncertainties of the X-ray and optical imaging (column 8). Note that the positional uncertainties for these clusters are all larger than the measurement uncertainties due to Poisson noise. The measured offsets are all less than roughly 20 kpc with the exception of AS0592 with an offset of 119.6 kpc. Upon further inspection of this outlier, it was determined to be a merging cluster.

Name	Catalogue	*Chandra* ObsID	z	Offset (kpc)	Error (kpc)	R_{500} (Mpc)	λ	Concentration	Position uncertainty (kpc)
RXCJ0232.2 − 4420	DES Y3	4993	0.28	17.7	1.3	1.44	117.47	0.51	5.38
MS 0906.5+1110	SDSS	924	0.18	16.0	0.4	1.23	174.7	0.53	3.24
A2445	SDSS	12 249	0.17	5.4	0.7	1.04	49.55	0.54	2.94
RXC J0532.9 − 3701	DES Y3	15 112	0.15	4.7	0.7	1.51	199.43	0.55	2.72
AS0592	DES Y3	16 572	0.25	119.6	0.4	1.51	96.37	0.57	4.56
A853	SDSS	12 250	0.27	4.5	0.7	0.94	50.21	0.59	5.14
RXJ1000.5+4409	SDSS	9421	0.17	11.3	0.6	0.85	27.42	0.6	3.04
RXCJ0220.9 − 3829	DES Y3	9411	0.23	7.9	0.8	0.93	53.37	0.62	4.34
RXCJ0307.0 − 2840	DES Y3	9414	0.18	19.3	0.8	1.33	102.58	0.62	3.14
A586	SDSS	530	0.25	20.6	0.6	1.3	120.09	0.74	4.71
RXC J2129.6+0005	DES Y3	9370	0.25	3.1	0.5	1.21	76.58	0.8	4.73
ABELL 2009	SDSS	10 438	0.19	7.0	0.4	1.24	91.82	0.91	3.39
RXCJ0331.1 − 2100	DES Y3	10 790	0.25	3.3	0.5	1.01	64.75	0.99	4.73
ZwCl 3146	SDSS	909	0.27	13.0	0.2	1.19	73.53	1.0	5.09
4C+55.16	SDSS	4940	0.16	6.8	0.3	1.1	46.82	1.0	2.83
A1835	SDSS	6880	0.18	11.4	0.1	1.35	134.28	1.07	3.17
A383	SDSS	2320	0.16	2.2	0.3	1.02	80.28	1.17	2.83
RXJ1720.1+2638	SDSS	4361	0.17	9.6	0.2	1.25	63.72	1.19	3.07
ZwCl 0348	DES Y3	10 465	0.19	11.8	0.2	0.83	49.28	1.28	3.34
ZwCl 2089	SDSS	10 463	0.29	1.6	0.2	0.88	27.08	1.29	5.56
MS1455.0+2232	SDSS	4192	0.24	7.7	0.2	1.04	54.92	1.35	4.48
RXC J0132.6 − 0804	DES Y3	16 149	0.26	9.8	0.7	0.7	27.74	1.56	4.81
ABELL 1204	SDSS	2205	0.28	1.7	0.2	0.92	39.82	1.88	5.35

concentration cut was not conservative enough to remove all merging clusters in non-simulated data.

Accordingly, we re-cut the data with a concentration of 0.6, which removed the merging cluster along with five other clusters. With this cut, the offsets range between 1.5 and 20.5 kpc, with most offsets falling between 4 and 15 kpc. A lognormal fit to the offset distribution for this more conservative sample resulted in a median value of 6.8 ± 1.3 kpc; the distribution and fit are both shown in the lower panel of Fig. 1.

4 DISCUSSION

Our results indicate a non-zero offset between the central galaxy and X-ray centre in our relaxed cluster sample even for our more conservative cut on concentration. As already noted, the offsets in all cases are significantly larger than the estimated uncertainty from Poisson noise. We now consider the accuracy of the positions of both *Chandra* X-ray sources and the central galaxies. For *Chandra*, the absolute positional accuracy when comparing measured point source X-ray centroids to optical or radio counterparts with well-measured positions is ∼0.7 arcsec (68 per cent).[1] In comparison, the DES Y3 Gold average absolute astrometric accuracy is 0.158 arcsec (Sevilla-Noarbe et al. 2021). Comparing the SEXTRACTOR (Bertin & Arnouts 1996) and NGMIX (Sevilla-Noarbe et al. 2021) estimated positions for the DES central galaxies in our sample, we find an average difference of 0.18 arcsec and use this as an estimate of the modelling uncertainties. Adding these in quadrature, gives an estimated central galaxy position uncertainty of 0.24 arcsec. Taken together the X-ray and optical positional uncertainties imply an uncertainty on the measured offsets of 0.74 arcsec, where we take .

In all but six cases, the measured offsets are larger than the positional uncertainty at the cluster redshift, though for a few additional clusters the offset and resolution are comparable. For the 17 clusters with concentration greater than 0.6, the average positional uncertainty is 4.0 kpc, ranging from 2.7 to 5.6 kpc. To account for this, we simulate the addition of positional uncertainties on separations of 4 kpc, finding the best fit difference between the true separation μ_t and the measured separation μ_m as $\mu_t^2 = \mu_m^2 - (4.0\,\mathrm{kpc}/a)^2$. We find the best fit $a \approx \sqrt{\pi/2}$. Using this formula and a $\mu_m = 6.8 \pm 1.3$ kpc, gives $6.0^{+1.4}_{-1.5}$ kpc. For the less conservative concentration cut of 0.5 after accounting for the positional uncertainty, we find a $\mu_m = 7.9 \pm 1.6$ kpc, for an average offset of $\mu = 7.2^{+1.7}_{-1.8}$ kpc.

In comparison, Harvey et al. (2019) similarly fit a lognormal to the distribution of CCG offsets for relaxed clusters in their simulations; they find that SIDM with a self-interacting cross-section of 1.0 $\mathrm{cm^2\,g^{-1}}$ has a μ-value of 8.6 ± 0.7 kpc, while a self-interacting cross-section of 0.3 $\mathrm{cm^2\,g^{-1}}$ gives a μ-value of 6.1 ± 0.7 kpc and CDM a μ-value of 3.8 ± 0.7 kpc. These median offsets are much smaller than the offsets predicted by the simulations from Kim et al. (2017), which were dark matter only. However, the quoted offsets from Harvey et al. (2019) are the initial results from their simulations before they accounted for numerical effects. They attempt to model the effects of the limited resolution of their simulations (softening length $\epsilon = 4h^{-1}$ kpc) using much smaller cluster samples taken from higher resolution simulations of two models, CDM and SIDM with cross-section 1.0 $\mathrm{cm^2\,g^{-1}}$. Their nominal results give a resolution

[1]Chandra Proposers' Observatory Guide, Cycle 24: https://cxc.harvard.edu/proposer/POG/html/index.html

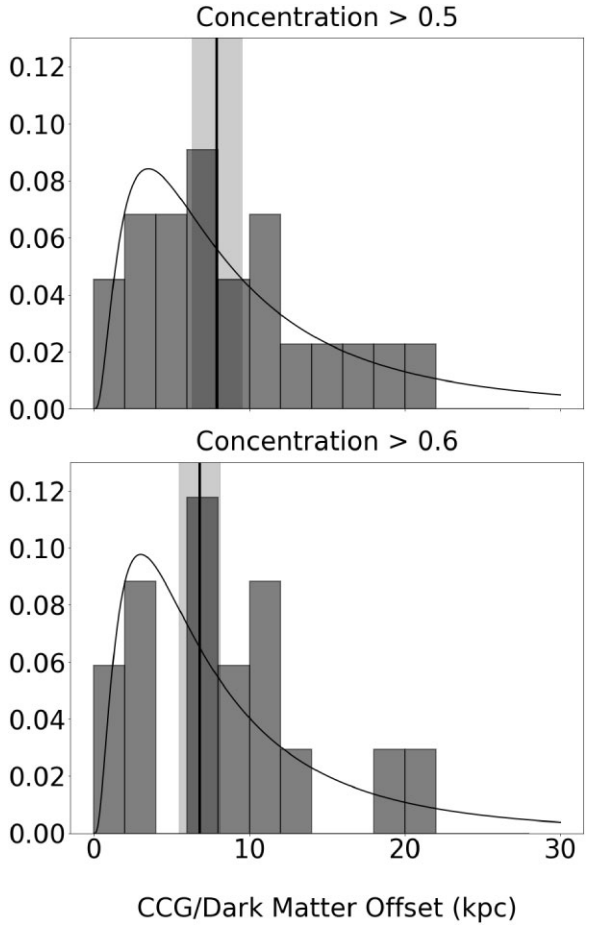

Figure 1. Histogram of CCG offsets from the calculated X-ray centroids for a concentration cut of 0.5 (top) and 0.6 (bottom). Also shown are the best-fitting lognormal distribution (black solid line) with $\mu = 7.9 \pm 1.6$ and 6.8 ± 1.3 kpc for the 0.5 and 0.6 concentration cuts, respectively. Vertical black lines and shaded region show the best-fitting μ and 1σ uncertainties estimated through bootstrapping.

Table 2. Results from fitting the offsets to a lognormal probability density function with parameters μ for the median value and σ for the variance. Errors on the model parameters were found via bootstrapping.

Concentration minimum	μ (kpc)	Bootstrap error	σ	Bootstrap error
0.5	7.9	1.6	0.9	0.2
0.6	6.8	1.3	0.8	0.1

corrected $\mu = 0.8^{+0.9}_{-0.8}$ kpc for CDM and $\mu = 2.3^{+1.8}_{-0.7}$ kpc for SIDM 1.0 cm^2 g^{-1}. They go on to derive a limit on the cross-section of σ/m < 0.4 cm^2 g^{-1} using the CCG offsets in 10 strong lensing clusters (Harvey et al. 2019). However, these numbers and comparisons to our results come with several important caveats. In particular, the resolution correction relies on small samples (∼20) of clusters run at higher resolution for only two different dark matter models. In addition, the high-resolution simulations lead to different inner stellar density profiles in the simulated clusters mixing baryonic and dark matter effects. The model for the resolution correction used is thus not well constrained nor particularly well motivated. Finally, our results are for the offset between the X-ray centre and central galaxy, which is not directly what is measured in the simulations. In addition, the BAHAMAS simulations used in Harvey et al. (2019) represent one implementation of baryonic physics, and more work is needed on the simulation side to understand how variations in the baryonic physics affect the central galaxy offsets. Studies such as Cui et al. (2016) and Seppi et al. (2023) demonstrate an effort to understand the connection between X-ray centres, central galaxies, and the halo centres of mass. In order to make useful constraints on SIDM cross-section given this data, these studies must be extended to non-ΛCDM models to compare directly with our results.

In general, our measurement of central galaxy offsets on the scale of several kpc are consistent with the expectations for a non-negligible SIDM cross-section on the order of ∼1.0 cm^2 g^{-1} and mildly in tension with the resolution-corrected CDM expectation (Harvey et al. 2019). However, given the caveats above we cannot rule out CDM. More work on the simulation side is needed to fully utilize and interpret our results, which is beyond the scope of the current paper. Our results are also compatible with current constraints on the SIDM cross-section. For example, Sagunski et al. (2021) find an upper limit on a velocity dependent cross section in clusters of σ/m < 0.35 cm^2 g^{-1} considering the measured inner densities of strong lensing clusters and groups (see also Newman et al. 2013). Considering a range of observations, Tulin & Yu (2018) conclude that a cross-section $\sigma/m \sim 0.5$–1 cm^2 g^{-1} could resolve small-scale structure problems while staying roughly consistent with large-scale structure constraints. However, they find that dwarf and low surface brightness galaxy observations imply cross-sections of $\sigma/m > 1$ cm^2 g^{-1}, and generally some velocity dependence of the self-interaction cross-section is preferred to reconcile cluster observations with smaller scales.

5 CONCLUSIONS

We use a combination of *Chandra* X-ray data and optical imaging from the DES and SDSS surveys to investigate the presence of offsets between cluster central galaxies and the cluster gravitational centre that are predicted to exist in models of dark matter including dark matter self-interactions. We use a cut on X-ray concentration to select relatively relaxed clusters and a redshift cut to ensure sufficient spatial resolution, resulting in a sample of 23 clusters.

We measured the offset between the centroid of X-ray emission and the CCG. Modelling the distribution of offsets with a lognormal distribution, we found the median value of the offset to be $\mu = 7.9 \pm 1.6$ kpc. As our initial concentration cut allowed one clear merger to remain in the sample, we also explored a more restrictive cut, resulting in a sample of 17 clusters. We found the median value of the offset for this sample to be $\mu = 6.8 \pm 1.3$ kpc. Our results indicate non-zero offsets for most clusters in the sample. Using Monte Carlo resimulations of the noise, we find that the uncertainty in the X-ray positions due to noise are typically an order of magnitude smaller than the measured offsets, with an average uncertainty of 0.5 kpc. Uncertainties in the absolute astrometry of both the X-ray and optical observations are larger, but still lower than the measured offsets for most of the clusters in our sample. Taking the more conservative concentration cut and accounting for the average positional uncertainties in both the X-ray and galaxy positions, results in an estimated median offset of $\mu = 6.0^{+1.4}_{-1.5}$ kpc.

Regardless of the concentration cut made, our results are consistent with some level of dark matter self-interaction of $\sigma/m \sim 1.0$ cm^2 g^{-1} when compared to the simulated results for relaxed clusters from Harvey et al. (2019), but we also cannot completely rule out CDM

given uncertainties in the simulated results and our use of the X-ray centre as a proxy for the dark matter position. In the future, these constraints can be improved by expanding the cluster sample size, in particular with additional ∗∗high-resolution X-ray observations of DES and SDSS clusters, and through the development of simulations which more directly simulate the measurements and cuts made here.

ACKNOWLEDGEMENTS

This work was supported by the U.S. Department of Energy under award number DE-SC0010107. Funding for the DES Projects has been provided by the U.S. Department of Energy, the U.S. National Science Foundation, the Ministry of Science and Education of Spain, the Science and Technology Facilities Council of the United Kingdom, the Higher Education Funding Council for England, the National Center for Supercomputing Applications at the University of Illinois at Urbana-Champaign, the Kavli Institute of Cosmological Physics at the University of Chicago, the Center for Cosmology and Astro-Particle Physics at the Ohio State University, the Mitchell Institute for Fundamental Physics and Astronomy at Texas A&M University, Financiadora de Estudos e Projetos, Fundação Carlos Chagas Filho de Amparo à Pesquisa do Estado do Rio de Janeiro, Conselho Nacional de Desenvolvimento Científico e Tecnológico and the Ministério da Ciência, Tecnologia e Inovação, the Deutsche Forschungsgemeinschaft, and the Collaborating Institutions in the Dark Energy Survey.

The Collaborating Institutions are Argonne National Laboratory, the University of California at Santa Cruz, the University of Cambridge, Centro de Investigaciones Energéticas, Medioambientales y Tecnológicas-Madrid, the University of Chicago, University College London, the DES-Brazil Consortium, the University of Edinburgh, the Eidgenössische Technische Hochschule (ETH) Zürich, Fermi National Accelerator Laboratory, the University of Illinois at Urbana-Champaign, the Institut de Ciències de l'Espai (IEEC/CSIC), the Institut de Física d'Altes Energies, Lawrence Berkeley National Laboratory, the Ludwig-Maximilians Universität München and the associated Excellence Cluster Universe, the University of Michigan, NSF's NOIRLab, the University of Nottingham, The Ohio State University, the University of Pennsylvania, the University of Portsmouth, SLAC National Accelerator Laboratory, Stanford University, the University of Sussex, Texas A&M University, and the OzDES Membership Consortium.

Based in part on observations at Cerro Tololo Inter-American Observatory at NSF's NOIRLab (NOIRLab Prop. ID 2012B-0001; PI: J. Frieman), which is managed by the Association of Universities for Research in Astronomy (AURA) under a cooperative agreement with the National Science Foundation.

The DES data management system is supported by the National Science Foundation under grant nos AST-1138766 and AST-1536171. The DES participants from Spanish institutions are partially supported by MICINN under grants ESP2017-89838, PGC2018-094773, PGC2018-102021, SEV-2016-0588, SEV-2016-0597, and MDM-2015-0509, some of which include ERDF funds from the European Union. IFAE is partially funded by the CERCA program of the Generalitat de Catalunya. Research leading to these results has received funding from the European Research Council under the European Union's Seventh Framework Program (FP7/2007-2013) including ERC grant agreements 240672, 291329, and 306478. We acknowledge support from the Brazilian Instituto Nacional de Ciência e Tecnologia (INCT) do e-Universo (CNPq grant 465376/2014-2).

This manuscript has been authored by Fermi Research Alliance, LLC under contract no. DE-AC02-07CH11359 with the U.S. Department of Energy, Office of Science, Office of High Energy Physics.

DATA AVAILABILITY

The offsets and other measurements made in this paper are included in Table 1. The DES and SDSS data underlying this paper are available at https://des.ncsa.illinois.edu/releases/dr2/dr2-docs and https://www.sdss3.org/dr8/, and all *Chandra* data used is in the public archive. The SDSS REDMAPPER catalogue is available through the VizieR service here: https://vizier.cds.unistra.fr/viz-bin/VizieR-3?-source=J/ApJS/224/1/cat_dr8; the DES Y3 REDMAPPER catalogue used is proprietary to the DES Collaboration, but will be released upon publication of the Y3 cluster cosmology papers.

REFERENCES

Adhikari S. et al., 2022, preprint (arXiv:2207.10638)
Aihara H. et al., 2011, ApJS, 193, 29
Bertin E., Arnouts S., 1996, A&AS, 117, 393
Bode P., Ostriker J. P., Turok N., 2001, ApJ, 556, 93
Botteon A., Gastaldello F., Brunetti G., 2018, MNRAS, 476, 5591
Buckley M. R., Peter A. H. G., 2018, Phys. Rep., 761, 1
Bullock J. S., Boylan-Kolchin M., 2017, ARA&A, 55, 343
Burkert A., 1995, ApJ, 447, L25
Casertano S., van Gorkom J. H., 1991, AJ, 101, 1231
Creasey P., Sameie O., Sales L. V., Yu H.-B., Vogelsberger M., Zavala J., 2017, MNRAS, 468, 2283
Cui W. et al., 2016, MNRAS, 456, 2566
Davis M., Efstathiou G., Frenk C. S., White S. D. M., 1985, ApJ, 292, 371
de Blok W. J. G., McGaugh S. S., Bosma A., Rubin V. C., 2001b, ApJ, 552, L23
de Blok W. J. G., McGaugh S. S., Rubin V. C., 2001a, AJ, 122, 2396
DES Collaboration, 2005, preprint (arXiv:astro-ph/0510346)
Dubinski J., Carlberg R. G., 1991, ApJ, 378, 496
Eisenstein D. J. et al., 2011, AJ, 142, 72
Flores R. A., Primack J. R., 1994, ApJ, 427, L1
Flores R., Primack J. R., Blumenthal G. R., Faber S. M., 1993, ApJ, 412, 443
Governato F. et al., 2010, Nature, 463, 203
Harvey D., Robertson A., Massey R., McCarthy I. G., 2019, MNRAS, 488, 1572
Hollowood D. L. et al., 2019, ApJS, 244, 22
Hu W., Barkana R., Gruzinov A., 2000, Phys. Rev. Lett., 85, 1158
Hui L., 2021, ARA&A, 59, 247
Hui L., Ostriker J. P., Tremaine S., Witten E., 2017, Phys. Rev. D, 95, 043541
Kamada A., Kaplinghat M., Pace A. B., Yu H.-B., 2017, Phys. Rev. Lett., 119, 111102
Kaplinghat M., Tulin S., Yu H.-B., 2016, Phys. Rev. Lett., 116, 041302
Khoury J., 2016, Phys. Rev. D, 93, 103533
Kim S. Y., Peter A. H. G., Wittman D., 2017, MNRAS, 469, 1414
Kuzio de Naray R., Martinez G. D., Bullock J. S., Kaplinghat M., 2010, ApJ, 710, L161
Kuzio de Naray R., McGaugh S. S., de Blok W. J. G., 2008, ApJ, 676, 920
Moore B., 1994, Nature, 370, 629
Navarro J. F., Frenk C. S., White S. D. M., 1996, ApJ, 462, 563
Navarro J. F., Frenk C. S., White S. D. M., 1997, ApJ, 490, 493
Newman A. B., Treu T., Ellis R. S., Sand D. J., 2013, ApJ, 765, 25
Oh S.-H., Brook C., Governato F., Brinks E., Mayer L., de Blok W. J. G., Brooks A., Walter F., 2011, AJ, 142, 24
Oman K. A. et al., 2015, MNRAS, 452, 3650
Ren T., Kwa A., Kaplinghat M., Yu H.-B., 2019, Phys. Rev. X, 9, 031020
Rykoff E. S. et al., 2014, ApJ, 785, 104
Rykoff E. S. et al., 2016, ApJS, 224, 1
Sagunski L., Gad-Nasr S., Colquhoun B., Robertson A., Tulin S., 2021, J. Cosmol. Astropart. Phys., 2021, 024

Seppi R. et al., 2023, A&A, 671, A57
Sevilla-Noarbe I. et al., 2021, ApJS, 254, 24
Spergel D. N., Steinhardt P. J., 2000, Phys. Rev. Lett., 84, 3760
Springel V. et al., 2005, Nature, 435, 629
Tulin S., Yu H.-B., 2018, Phys. Rep., 730, 1
Viel M., Becker G. D., Bolton J. S., Haehnelt M. G., 2013, Phys. Rev. D, 88, 043502
Weinberg D. H., Bullock J. S., Governato F., Kuzio de Naray R., Peter A. H. G., 2015, Proc. Natl. Acad. Sci., 112, 12249
Zavala J., Lovell M. R., Vogelsberger M., Burger J. D., 2019, Phys. Rev. D, 100, 063007
Zhang Y. et al., 2019, MNRAS, 487, 2578
Zolotov A. et al., 2012, ApJ, 761, 71

[1]*Physics Department, UC Santa Cruz, 1156 High Street, Santa Cruz, CA 95064, United States*
[2]*Santa Cruz Institute for Particle Physics, Santa Cruz, CA 95064, USA*
[3]*Institute of Space Sciences (ICE, CSIC), Campus Universitat Aut−onoma de Barcelona, Carrer de Can Magrans, s/n, E-08193 Barcelona, Spain*
[4]*Department of Physics and Astronomy, San Francisco State University, 1600 Holloway Ave, San Francisco, CA 94132, USA*
[5]*Department of Physics, Indian Institute of Science Education and Research Pune, Pune 411045, India*
[6]*Faculty of Physics, University Observatory, Ludwig-Maximilians-Universitat, Scheinerstr. 1, D-81679 Munich, Germany*
[7]*SLAC National Accelerator Laboratory, 2575 Sand Hill Road, Menlo Park, CA 94025, USA*
[8]*Jet Propulsion Laboratory, California Institute of Technology, 4800 Oak Grove Dr, Pasadena, CA 91109, USA*
[9]*Department of Physics and Astronomy, Clemson University, Kinard Lab of Physics, Clemson, SC 29634-0978, USA*
[10]*Laboratório Interinstitucional de e-Astronomia - LIneA, Rua Gal. José Cristino 77, Rio de Janeiro, RJ - 20921-400, Brazil*
[11]*Department of Physics, University of Michigan, Ann Arbor, MI 48109, USA*
[12]*Institute of Cosmology and Gravitation, University of Portsmouth Portsmouth PO1 3FX, UK*
[13]*Institut d'Astrophysique de Paris, CNRS, UMR 7095, F-75014 Paris, France*
[14]*Institut d'Astrophysique de Paris, Sorbonne Universités, UPMC Univ Paris 06, UMR 7095, F-75014, Paris, France*
[15]*Department of Physics and Astronomy, University College London, Gower Street, London WC1E 6BT, UK*
[16]*Kavli Institute for Particle Astrophysics and Cosmology, Stanford University, PO Box 2450, Stanford, CA 94305, USA*
[17]*SLAC National Accelerator Laboratory, Menlo Park, CA 94025, USA*
[18]*Instituto de Astrofisica de Canarias, E-38205 La Laguna, Tenerife, Spain*
[19]*Departmento Astrofísica, Universidad de La Laguna, E-38206 La Laguna, Tenerife, Spain*
[20]*Center for Astrophysical Surveys, National Center for Supercomputing Applications, 1205 West Clark St., Urbana, IL 61801, USA*
[21]*Department of Astronomy, University of Illinois at Urbana-Champaign, 1002 W. Green Street, Urbana, IL 61801, USA*
[22]*Physics Department, William Jewell College, Liberty, MO 64068, USA*
[23]*Astronomy Unit, Department of Physics, University of Trieste, via Tiepolo 11, I-34131 Trieste, Italy*
[24]*INAF – Osservatorio Astronomico di Trieste, via G. B. Tiepolo 11, I-34143 Trieste, Italy*
[25]*Institute for Fundamental Physics of the Universe, Via Beirut 2, I-34014 Trieste, Italy*
[26]*Hamburger Sternwarte, Universität Hamburg, Gojenbergsweg 112, D-21029 Hamburg, Germany*
[27]*School of Mathematics and Physics, University of Queensland, Brisbane, QLD 4072, Australia*
[28]*Department of Physics, IIT Hyderabad, Kandi, Telangana 502285, India*
[29]*Institute of Theoretical Astrophysics, University of Oslo, PO Box 1029 Blindern, NO-0315 Oslo, Norway*
[30]*Fermi National Accelerator Laboratory, PO Box 500, Batavia, IL 60510, USA*
[31]*Kavli Institute for Cosmological Physics, University of Chicago, Chicago, IL 60637, USA*
[32]*Instituto de Fisica Teorica UAM/CSIC, Universidad Autonoma de Madrid, E-28049 Madrid, Spain*
[33]*Institut de Física d'Altes Energies (IFAE), The Barcelona Institute of Science and Technology, Campus UAB, E-08193 Bellaterra (Barcelona), Spain*
[34]*Faculty of Physics, Ludwig-Maximilians-Universität, University Observatory, Scheinerstr. 1, D-81679 Munich, Germany*
[35]*Center for Cosmology and Astro-Particle Physics, The Ohio State University, Columbus, OH 43210, USA*
[36]*Department of Physics, The Ohio State University, Columbus, OH 43210, USA*
[37]*Center for Astrophysics | Harvard & Smithsonian, 60 Garden Street, Cambridge, MA 02138, USA*
[38]*Australian Astronomical Optics, Macquarie University, North Ryde, NSW 2113, Australia*
[39]*Lowell Observatory, 1400 Mars Hill Rd, Flagstaff, AZ 86001, USA*
[40]*George P. and Cynthia Woods Mitchell Institute for Fundamental Physics and Astronomy, and Department of Physics and Astronomy, Texas A&M University, College Station, TX 77843, USA*
[41]*Centro de Investigaciones Energéticas, Medioambientales y Tecnológicas (CIEMAT),Madrid, 28040, Spain*
[42]*Institució Catalana de Recerca i Estudis Avançats, E-08010 Barcelona, Spain*
[43]*Observatório Nacional, Rua Gal. José Cristino 77, Rio de Janeiro, RJ - 20921-400, Brazil*
[44]*Department of Astrophysical Sciences, Princeton University, Peyton Hall, Princeton, NJ 08544, USA*
[45]*Department of Physics, University of Genova and INFN, Via Dodecaneso 33, I-16146 Genova, Italy*
[46]*Department of Physics and Astronomy, Pevensey Building, University of Sussex, Brighton BN1 9QH, UK*
[47]*School of Physics and Astronomy, University of Southampton, Southampton SO17 1BJ, UK*
[48]*Instituto de Física Gleb Wataghin, Universidade Estadual de Campinas, 13083-859, Campinas, SP, Brazil*
[49]*Computer Science and Mathematics Division, Oak Ridge National Laboratory, Oak Ridge, TN 37831, USA*
[50]*National Center for Supercomputing Applications, 1205 West Clark St,Urbana, IL 61801, USA*
[51]*Lawrence Berkeley National Laboratory, 1 Cyclotron Road, Berkeley, CA 94720, USA*
[52]*Max Planck Institute for Extraterrestrial Physics, Giessenbachstrasse, D-85748 Garching, Germany*
[53]*Fakultät für Physik, Ludwig-Maximilians Universität München, Universitäts-Sternwarte, Scheinerstr. 1, D-81679 München, Germany*

This paper has been typeset from a TEX/LATEX file prepared by the author.